J Mater Sci (2006) 41:5424–5428
DOI 10.1007/s10853-006-0258-6

Agglomeration control of hydroxyapatite nano-crystals grown in phase-separated microenvironments

Kimiyasu Sato · Yuji Hotta · Takaaki Nagaoka · Masaki Yasuoka · Koji Watari

Received: 3 March 2005 / Accepted: 18 October 2005 / Published online: 13 June 2006

Abstract Materials synthesis processes that require high temperatures consume large quantities of energy that generate an environmental burden. We attempted to synthesize hydroxyapatite (HAp) nano-crystals without firing or melting. ''Water in oil'' (W/O) emulsions were employed as microreactors for HAp formation. The surfactant-bounded water mediated HAp crystal nucleation, and HAp nano-crystallites were obtained. The obtained particles were aggregates composed of plate-like nano-crystals and monodisperse tiny crystals. Utilization of the W/O emulsions resulted in tunable nucleation frequency and the reactant provision, and yielded HAp nano-crystals with characteristic agglomeration properties.

Introduction

Due to similarities with the mineral constituents of bones and teeth, hydroxyapatite (HAp), $Ca_{10}(PO_4)_6(OH)_2$, is one of the most biocompatible materials known [1]. HAp contains only nontoxic species that should dissolve in the human body without any apparent risk to health [2]. Nano-sized HAp crystals are thought to be suitable for use in various medical materials; for instance, drug delivery systems (DDS), protein delivery systems, artificial organs and scaffolds for tissue engineering. HAp nano-crystals also have the potential to immobilize environmentally harmful materials [3]. The surface structure of the HAp crystal has recently been determined [4], and the knowledge gained in this study should help promote the use of HAp nano-crystals. We attempted in this investigation to synthesize HAp nano-crystals without firing or melting. Processes that require high temperatures consume large quantities of energy that place a burden on environment. The biomineralization process (the formation of inorganic crystals in living bodies) proceeds at ambient temperature. Mimicking biomineralization is likely to be the most environment-friendly synthesis process [5]. In biomineralization, organic supramolecular systems are used as pre-organized environments to control the formation of finely divided inorganic materials [6, 7]. In the present paper, we attempt to synthesize HAp nano-crystals using a bio-inspired method.

Phase-separated microenvironments provided by ''Water in oil'' (W/O) emulsions have been utilized as vesicles for the synthesis of fine ceramic powders [8], and there are several reports on the use of emulsions for the synthesis of HAp nano-crystals [9–12]. Crystallization in emulsions is known to occur by nucleation and growth of crystals within the emulsion droplets, and nucleation often takes place at the droplet surfaces. It has been reported that negatively charged organic functional groups can induce heterogeneous nucleation of HAp crystals [13–16]. The W/O emulsion structure possesses large interfaces between aqueous solutions (the crystal growth media) and organic matrices with functional groups. We employed the W/O emulsion structure as an artificial organic template to reproduce the organic supramolecular systems in natural bodies.

It is desirable to preselect the HAp nano-crystals' agglomeration states between mono-dispersed types and

K. Sato (✉) · Y. Hotta · T. Nagaoka · M. Yasuoka · K. Watari
National Institute of Advanced Industrial Science and Technology (AIST), Anagahora 2266-98, Shimoshidami, Moriyama-ku, Nagoya 463-8560, Japan
e-mail: sato.kimiyasu@aist.go.jp

agglomerates in a house-of-cards structure, according to the planned application of the nano-materials. The former can be utilized as pharmaceuticals or biomaterials without further modification, and the latter as DDS carriers whose pores can store drugs [2]. The heating and drying processes of as-prepared HAp nano-crystals often result in enlargement and agglomeration of the particles. We attempted to achieve a process that can yield HAp nano-crystals in the desired agglomeration states without a heating process.

Experimental

Sodium bis(2-ethylhexyl)sulfosuccinate (AOT), $NaO_3SCH(COOC_8H_{17})CH_2COOC_8H_{17}$, and cyclohexane ($C_6H_{12}$) were used as the oil phase of the emulsion. AOT is the most widely employed surfactant for W/O emulsions, since it is known to form stable reverse micelles over a wide range of water/surfactant mole ratios [8]. AOT was purchased from Tokyo Kasei Kogyo Co., Japan, and was used without further purification. C_6H_{12}, calcium hydroxide [$Ca(OH)_2$], and potassium dihydrogen phosphate (KH_2PO_4) were purchased from Wako Pure Chemical Industries Ltd., Japan, and were used without further purification. Water was distilled and ion-exchanged before use. $Ca(OH)_2$ aqueous suspension was added to C_6H_{12} containing AOT while stirring vigorously. AOT possesses a sulfo group in its structure and acts as an anionic surfactant. The mixture was aged for 1 h, after which KH_2PO_4 aqueous solution was added. In surfactant–oil–water systems, water is readily solubilized to form small water-pools surrounded by the surfactant molecules. These phase-separated microenvironments, i.e., microemulsions, were utilized as microreactors for crystal nucleation and growth. The reactions were conducted for 72 h under intense agitation. All the processes were conducted at a fixed temperature of 25 °C. The resulting materials were separated by centrifugation, then washed with water and ethanol, and dried at ambient temperature.

The region of existence of W/O emulsion structures in a surfactant–oil–water system can be depicted in terms of a ternary phase diagram (Fig. 1). Water is readily incorporated into the polar core, forming a so-called ''water pool'' surrounded by AOT molecules. A microemulsion is an emulsion where the volume of water in the oil is small, so that the emulsion remains transparent. We tested two synthesis systems based on the obtained phase diagram, which we hereinafter designate as experimental systems (a) and (b). The concentrations and amounts of the reagents incorporated in the W/O emulsion system are given in Table 1, and the AOT–cyclohexane–water ratios employed are denoted by (a) and (b) in the phase diagram.

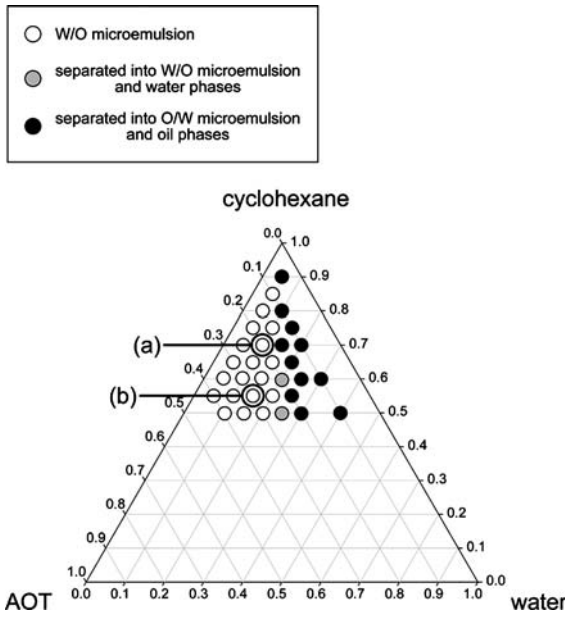

Fig. 1 The ternary phase diagram for AOT–cyclohexane–water at 25 °C

Table 1 Concentrations and amounts of the constituent chemicals for the experimental systems

	Concentration and amount			
	$Ca(OH)_2$	KH_2PO_4	C_6H_{12}	AOT
(a)	2.5 M/2.0 ml	1.5 M/2.0 ml	28.0 g	8.0 g
(b)	100 mM/3.0 ml	60 mM/3.0 ml	22.0 g	12.0 g

The structures of the emulsions during the crystallization process were evaluated using dynamic light scattering (DLS) equipment to accommodate dense specimens (FPAR-1000, Otsuka Electronics Co., Japan). X-ray diffraction (XRD) patterns of the obtained crystals were collected using a diffractometer (RINT-2550, Rigaku Co., Japan) using Cu-Kα radiation, operated at 40 kV and 400 mA. IR spectra were taken with a Fourier-transformed IR spectrometer (Spectrum GX, Perkin-Elmer, USA). The morphologies of the crystals were studied using a transmission electron microscope (TEM, JEM-2010, JEOL, Japan) operated at 200 kV.

Results and discussion

The microemulsion systems employed here are transparent when they contain neither $Ca(OH)_2$ nor KH_2PO_4, but the induction of the solutes into the emulsion systems drastically changed their structures. The water droplets became larger and made the emulsions translucent or opaque. Figure 2 shows the droplet size distribution of the W/O emulsions

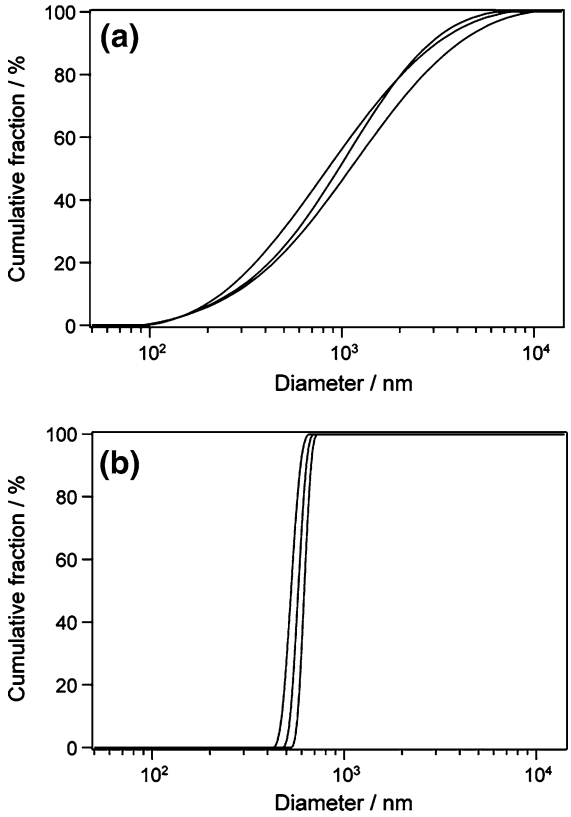

Fig. 2 Droplet size distribution profiles of the W/O emulsions evaluated by DLS for Experimental System (a) and (b). For each case, we measured three samples. The results are presented in a chart

incorporating $Ca(OH)_2$ and KH_2PO_4 as evaluated by DLS measurements. The size distribution profiles for Experiment System (a) showed gentle slopes, and the mean of the median droplet sizes from the three measurements was 980 nm. The size distribution profiles for Experiment System (b) were much steeper than those of (a) and the mean of the median droplet sizes was 570 nm. It is known that the emulsion structures depend not only on surfactant–oil–water ratios but vary in response to other factors. With higher ionic strength of the aqueous phase, the shrinkage of the electrical double layer at the water–oil interface and increase in the interface tension result in structural changes of the emulsions [17]. The addition of the solutes should encourage coalescence and change the size distributions of the emulsions.

Figure 3 shows the XRD patterns of the obtained crystals. Peaks that can be attributed to the apatite structure can be observed. The crystal structure of apatite is expressed in terms of the hexagonal symmetry. No crystalline phase (such as tricalcium phosphate) other than apatite is detected. The broadness of the diffraction peaks can be attributed to both the small size and low crystallinity of the obtained crystals. In the FT-IR spectra of the specimens (not shown), absorption due to OH stretching and libration were found. Stretching bands due to carbonate substitution

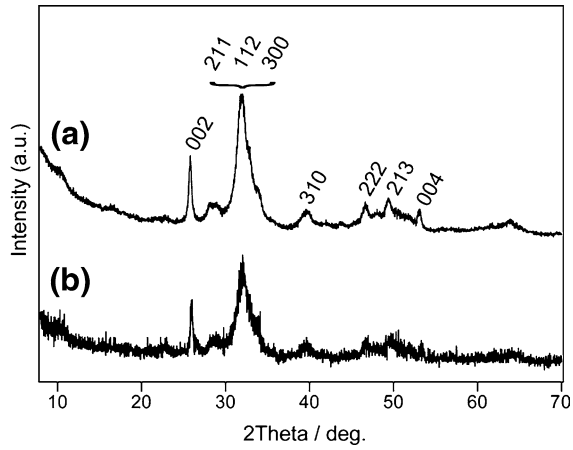

Fig. 3 X-ray diffraction patterns of the obtained crystals

of the phosphate positions in the apatite lattice were also observed. The carbonate ions derive from a reaction between atmospheric carbon dioxide and the solution. The precipitation products were revealed to be carbonate-containing HAp crystals.

The morphologies of the HAp crystals were investigated by TEM. As for Experiment System (a), the obtained crystals exhibit an elongated plate-like form of about 50–200 nm in length and about 10 nm thick (Fig. 4). The apparent elongated crystals are in plate-like form when viewed edge-on. They assembled to form aggregates that were 500 nm to 1 μm in diameter. High-resolution TEM (HRTEM) shows lattice fringes in the nano-crystals. The lattice-fringe image of the nano-crystals observed is shown in Fig. 4 together with its Fourier transform. The periodicity of the lattice fringe is 0.82 nm, which can be assigned to the interplanar spacing of {100} in the HAp structure. These spots are found in the direction vertical to the elongated form, indicating that the plate-like HAp single crystals are parallel to the {100} planes. Figure 5 shows the TEM photos of the HAp crystals obtained from Experiment System (b). Monodisperse HAp crystals in rectangular to rod-like shapes are found. The sizes of the crystals are much smaller than those of the crystals obtained in Experiment (a). HRTEM shows lattice fringes that can be assigned to the interplanar spacing of (002). These spots are found in the direction parallel to the elongated form, indicating that the HAp single crystals elongate parallel to their *c*-axes. We were thus able to arbitrarily switch the HAp nano-crystals' agglomeration states between mono-dispersed and agglomerated.

The solute content of emulsion droplets is rapidly exchanged through droplet collisions, formation of transient dimers, and breakdown of these transient dimers. As for reactions in W/O emulsions involving reactant species

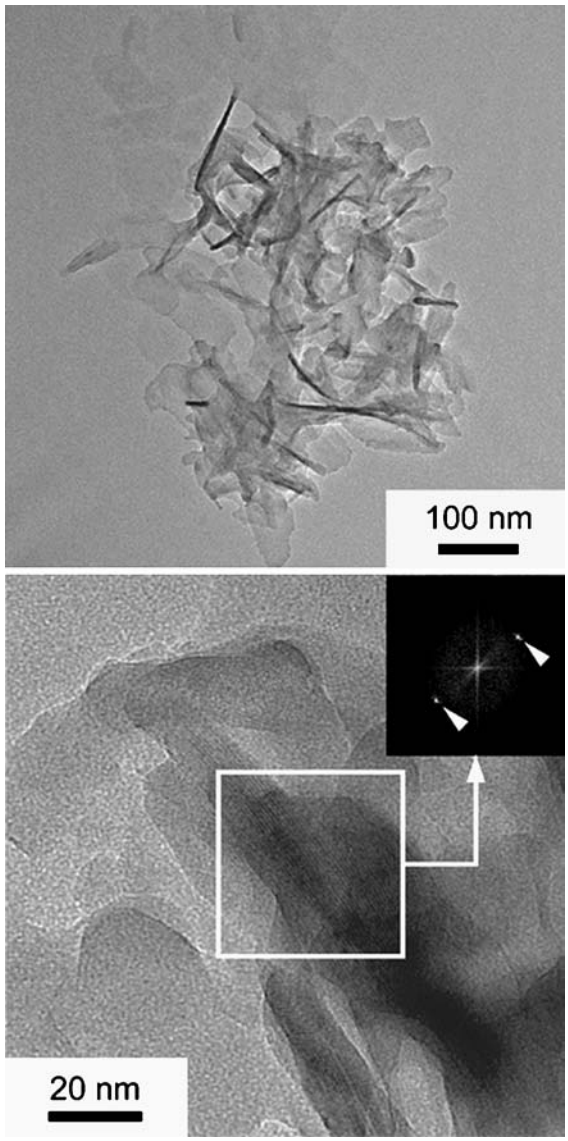

Fig. 4 (Top) TEM image of the HAp nano-crystals obtained from Experiment (a). (Bottom) HRTEM image of the crystals. Fourier transforms and the corresponding areas are also shown. Arrows in the Fourier transforms indicate the spots corresponding to 0.82 nm, which is ascribed to the interplanar spacing of {100} in HAp. The spots are found in the direction vertical to the elongated form

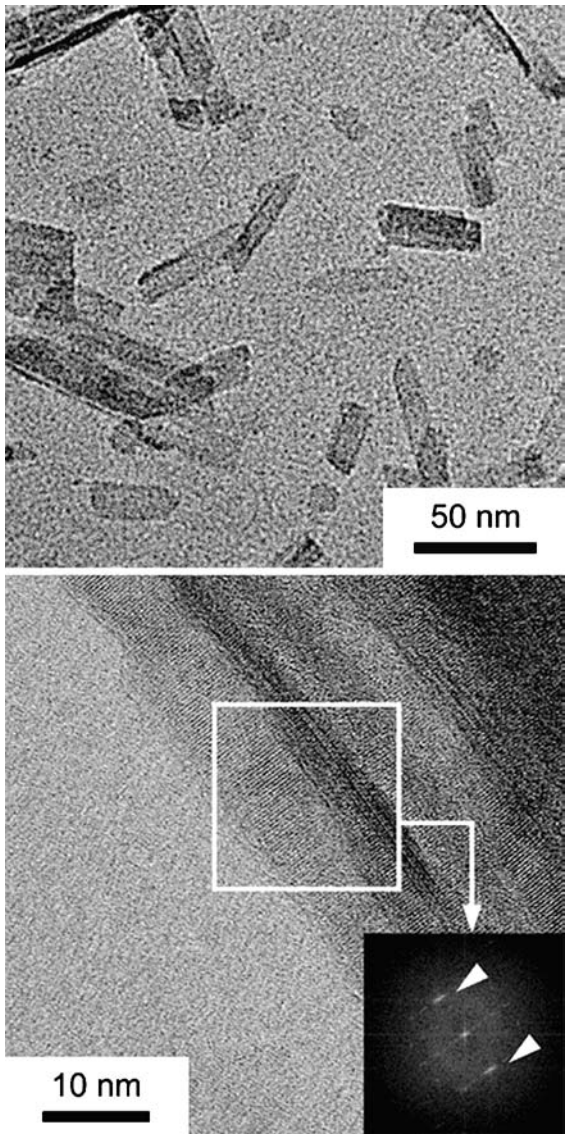

Fig. 5 (Top) TEM image of the HAp nano-crystals obtained from Experiment (b). (Bottom) HRTEM image of the crystals. Fourier transforms and the corresponding areas are also shown. Arrows in the Fourier transforms indicate the spots corresponding to 0.34 nm, which is ascribed to the interplanar spacing of (002) in HAp. The spots are found in the direction parallel to the elongated form

totally confined within the dispersed water droplets, a necessary step prior to their chemical reaction is transferring of the reactants into the same droplet. It has been reported that for rigid droplet-type structures such as that of AOT reverse micelles, one out of 10^4 encounters results in merging and solute exchange [8]. Provision of the reactants through the stable walls of the emulsions is much slower than diffusion of the solutes in bulky water, and slow provision of the reactants restricts crystal growth. On the other hand, as mentioned above, HAp nucleation can be induced by negatively charged functional groups on organic matrices. Heterogeneous nucleation occurs within the water droplet at the molecular wall, induced by the organic functional groups.

The balance between provision of the materials necessary for crystal growth and the frequency of crystals nucleation appears to be the key to controlling the sizes and agglomeration structures of the nano-crystals. Linking high frequency nucleation with slow provision should result in small primary particles. Of the two experiments presented in this work, the concentrations of the solutes in Experiment (a) are much larger that those of (b), and the [AOT]/[Ca^{2+}] molar ratio of Experiment (b) is

25 times higher than that of (a). In other words, Experiment (a) is characterized by higher supersaturation and the lower nucleation frequency. Once nucleation occurs, HAp crystal formation proceeds spontaneously within the water droplet. The inner portion of the aggregates is thought to be composed of HAp crystals grown in a homoepitaxial manner on the other HAp crystals. The crystals' maturation process results in the formation of agglomerates in house-of-cards structure. Experiment (b) is characterized by lower supersaturation and higher nucleation frequency. The crystal growth appears to be restricted and is prevented from making contact with the neighboring crystals. The resultant HAp crystals are monodisperse tiny ones. The inferred crystal maturation process is illustrated in Fig. 6.

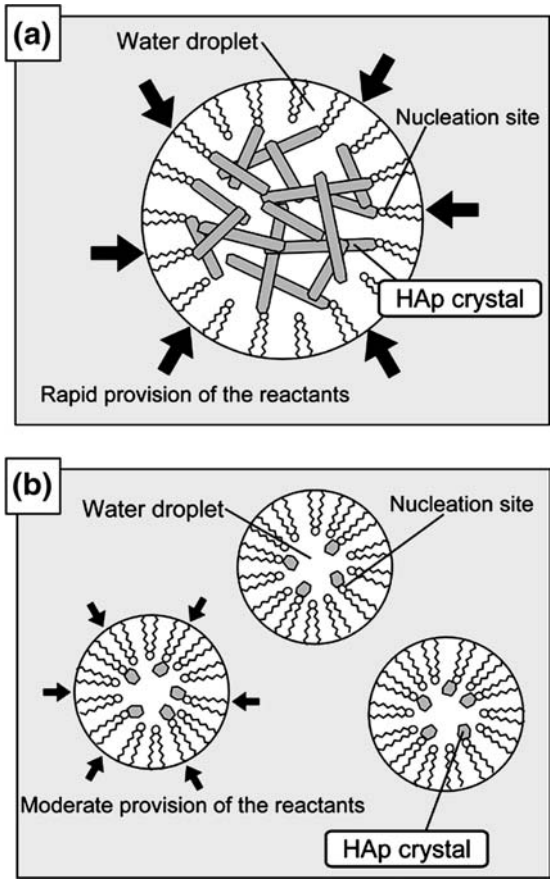

Fig. 6 Schema showing the inferred model of HAp nano-crystal formation

Conclusion

HAp nano-sized crystals were synthesized within W/O emulsions composed of AOT and C_6H_{12}. Heterogeneous nucleation can be induced by organic functional groups within the water droplets surrounded by the AOT molecular walls. By utilizing this method, it is possible to arbitrarily preselect the nano-crystals' agglomeration states between mono-dispersed versions and agglomerates. The obtained particles are aggregates composed of plate-like nano-crystals and monodisperse tiny ones. Controlled combination of the nucleation frequency and the reactant provision were achieved using W/O emulsion systems, and resulted in the formation of HAp nano-crystals with characteristic agglomeration properties.

References

1. Elliott JC (1994) Structure and chemistry of the apatite and other calcium orthophosphates. Elsevier, Amsterdam
2. Aoki H, Aoki H, Kutsuno T, Li W, Niwa M (2000) J Mater Sci Mater Med 11: 67
3. Watanabe Y, Moriyoshi Y, Suetsugu Y, Ikoma T, Kasama T, Hashimoto T, Yamada H, Tanaka J (2004) J Am Ceram Soc 87: 1395
4. Sato K, Kogure T, Iwai H, Tanaka J (2002) J Am Ceram Soc 85: 3054
5. Mann S (1996) Biomimetic materials chemistry. VCH Publishers, New York
6. Mann S (1996) In: Mann S, Webb J, Williams RJP (eds) Biomineralization: chemical and biochemical perspectives. VCH Publishers, New York, p 35
7. Mann S (2001) Biomineralization: principles and concepts in bioinorganic materials chemistry. Oxford University Press, Oxford
8. Adair JH, Li T, Kido T, Havey K, Moon J, Mecholsky J, Morrone A, Talham DR, Ludwig MH, Wang L (1998) Mater Sci Eng R-Rep 23: 139
9. Qi L, Ma J, Cheng H, Zhao Z (1997) J Mater Sci Lett 16: 1779
10. Furuzono T, Walsh D, Sato K, Sonoda K, Tanaka J (2001) J Mater Sci Lett 20: 111
11. Sonoda K, Furuzono T, Walsh D, Sato K, Tanaka J (2002) Solid State Ionics 151: 321
12. Phillips MJ, Darr JA, Luklinska ZB, Rehman I (2003) J Mat Sci: Mater Med 14: 875
13. Tanahashi M, Matsuda T (1997) J Biomed Mater Res 34: 305
14. Sato K, Kumagai Y, Tanaka J (2000) J Biomed Mater Res 50: 16
15. Sato K, Kogure T, Kumagai Y, Tanaka J (2001) J Colloid Interface Sci 240: 133
16. Sato K, Kumagai Y, Ikoma T, Watari K, Tanaka J (2005) J Ceram Soc Jpn 113: 112
17. Marinova KG, Alargova RG, Denkov ND, Velev OD, Petsev DN, Ivanov IB, Borwankar RP (1996) Langmuir 12: 2045